AD-A103 963 MAINE UNIV ORONO F/G 20/10
PERTURBATION THEORY FOR POLAR FLUIDS.(U)
JUL 81 J C RASAIAH N00014-78-C-0724
UNCLASSIFIED NL

LEVEL II

12

Final Report on

Perturbation Theory for Polar Fluids

Office of Naval Research

Contract N00014 78-c-0724

July 1981

Principal Investigator

J. C. Rasaiah

Institution

University of Maine

Orono, Maine 04469

b. Publication Citations

1. The adsorption of dipoles at a wall in the presence of an electric field: The RLHNC Approximation Journal of Chemical Physics 73, 3980, (1980). John M. Eggebrecht, Dennis J. Isbister and Jayendran C. Rasaiah.

2. Electrostriction and Dipolar Ordering at an Electrified Wall, Chemical Physics Letters 79, 189, (1981). J. C. Rasaiah, D. J. Isbister and G. Stell.

3. Nonlinear Effects in Polar Fluids. A Molecular Theory of Electrostriction. Journal of Chemical Physics (1981) - to appear. J. C. Rasaiah, D. J. Isbister and G. Stell.

c. Data on Scientific Collaborators

1. Mark Cilley - Programmer

2. John M. Eggebrecht - Graduate Student

3. Dennis J. Isbister - Postdoctoral Research Associate
(from Chemistry Department, Faculty of Military Studies, University of New South Wales, Duntroon, ACT, Australia)

4. Noel E. Thompson - Visiting Professor
(from Department of Mechanical Engineering, University of New South Wales, Duntroon, ACT, Australia)

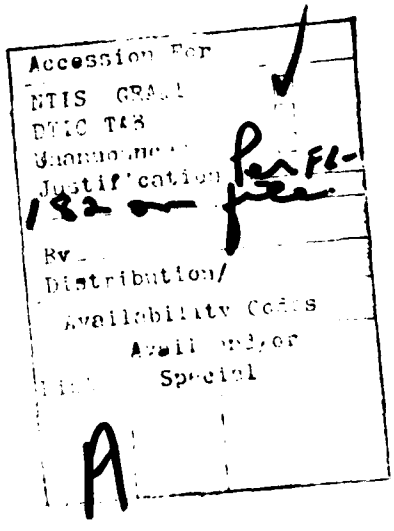

Summary

Work completed under this grant on polar fluids includes an extension of perturbation theory to polar molecules with point octopoles and hexadecapoles as well as a preliminary investigation of molecules with non-spherical cores. In addition, the ordering of dipolar molecules near a flat electrified wall has been investigated in the linearized hypernetted chain (LHNC) and quadratic hypernetted chain (QHNC) approximations. This has led to a new study of electrostriction and non-linear effects in the polarization density of dipolar fluids.

This report describes research on polar fluids carried out at the University of Maine at Orono under contract from the Office of Naval Research. Apart from the principal investigator (Professor J. C. Rasaiah), a visiting fellow, Professor Noel Thompson from Australia, a graduate student, Mr. John Eggebrecht and a postdoctoral fellow, Dr. Dennis Isbister from the Royal Military College, University of New South Wales in Australia, worked on this project; the last two receiving partial financial support under the present contract.

The primary objective of this investigation was to extend the theory of polar fluids developed by Stell, Rasaiah and Narang[1] to (a) spherical molecules with point-octopoles and point-hexadecapoles which could serve as a reasonable model for methane and sulfur hexafluoride; (b) non-spherical molecules with dipoles and/or quadrupoles such as HCN and O_2. A second objective was to extend our study of dipoles to surface adsorption near an electrified wall.

A Monte Carlo calculation of the free energy changes that accompany the switching on of polar interactions between the molecules was planned as an unambiguous test of the accuracy of the theory when applied to non-spherical cores. Some aspects of this work are still in progress, while parts (a) and (b) of the research described have been completed. In addition, a very promising and important theoretical investigation of the adsorption of dipoles at a wall in the presence of an electric field has been initiated with the assistance of Dr. Dennis Isbister and John Eggebrecht. In what follows, the research that has been completed with support from ONR is described in greater detail and future plans to continue this work are outlined.

I. Perturbation Theory for Polar Fluids

While the potential energies of interaction amongst point-dipoles and point-quadrupolesare well known, there are inconsistencies and ambiguities in the literature when higher order multipoles were included.[2] It was therefore decided to calculate these energies from first principles, limiting our attention only to octopolar and hexadecapolar interactions beyond quadrupolar charge distributions. It became necessary therefore to perform the tedious contractions of multipolar and field tensors the eight index field tensor for the hexadecapole-hexadecapole energy contains nearly 700 terms.[2] The two-body potentials beyond the simple dipole-dipole, dipole-quadrupole and quadrupole-quadrupole interactions were found to be

$$u_{ij}^{\mu\Omega} = \frac{\mu_i \Omega_j}{2r^5}\left[35\cos^3\theta_j\cos\theta_j\cos\theta_i - 15(\cos\theta_i\cos\theta_j+\cos^2\theta_j\cos\theta_{ij})+3\cos\theta_{ij}\right]$$

$$u_{ij}^{\Theta\Omega} = \frac{5\Theta_i \Omega_j}{4r^5}\left[63\cos^2\theta_i\cos^3\theta_j - 21\cos^2\theta_i - 42\cos\theta_i\cos^2\theta_j\cos\theta_{ij}+6[\cos\theta_j\cos^2\theta_{ij} + \cos\theta_i\cos\theta_{ij}]+3\cos\theta_j - 7\cos^3\theta_j\right]$$

$$u_{ij}^{\Omega\Omega} = \frac{-5\Omega_i \Omega_j}{4r_{ij}^7}\{231\cos^3\theta_i\cos^3\theta_j - 63[\cos^3\theta_i\cos\theta_j+\cos\theta_i\cos^3\theta_j + 3\cos^2\theta_i\cos^2\theta_j\cos\theta_{ij}] + 21[\cos^2\theta_i+\cos^2\theta_j+2\cos\theta_i\cos\theta_j\cos\theta_{ij}]\cos\theta_{ij}+21\cos\theta_i\cos\theta_j - 2\cos^3\theta_{ij} - 3\cos\theta_{ij}\}$$

$$u_{ij}^{\mu\Phi} = \frac{5\mu_i \Theta_j}{8r_{ij}^6}\{63\cos\theta_i\cos^4\theta_j - 42\cos\theta_i\cos^2\theta_j - 28\cos^3\theta_j\cos\theta_{ij}+3\cos\theta_i+12\cos\theta_i\cos\theta_{ij}\}$$

$$u_{ij}^{\Theta\Phi} = \frac{5\Theta_i\Phi_j}{16r_{ij}^7}\{693\cos^2\theta_i\cos^4\theta_j - 63[\cos^4\theta_j + 6\cos^2\theta_i\cos^2\theta_j + 8\cos\theta_i\cos^3\theta_j\cos\theta_{ij}] + 7[3\cos^2\theta_i + 6\cos^2\theta_j + 12\cos^2\theta_j\cos^2\theta_{ij} + 24\cos\theta_j\cos\theta_i\cos\theta_j\cos\theta_{ij} - 12\cos^2\theta_{ij} - 3]\}$$

$$u_{ij}^{\Omega\Phi} = -\frac{35\Omega_i\Phi_j}{16r_{ij}^8}\{429\cos^3\theta_i\cos^4\theta_j - 99[2\cos^3\theta_i\cos^2\theta_j + \cos\theta_i\cos^4\theta_j + 4\cos^2\theta_i\cos^3\theta_j\cos\theta_{ij}] + 9[\cos^3\theta_i + 12\cos^2\theta_i\cos\theta_j\cos\theta_{ij} + 6\cos\theta_i\cos^2\theta_j + 12\cos\theta_i\cos^2\theta_j\cos^2\theta_{ij} + 4\cos^3\theta_j\cos\theta_{ij}] - 12\cos\theta_i\cos^2\theta_{ij} - 3\cos\theta_i - 8\cos\theta_j\cos^3\theta_{ij} - 12\cos\theta_{ij}\cos^2\theta_{ij}\}$$

where μ, Θ, Ω, and Φ are the dipole, quadrupole, octopole and hexadecapole moments and

$$\cos\theta_{ij} = \cos\theta_i\cos\theta_j - \sin\theta_i\sin\theta_j\cos(\phi_i - \phi_j)$$

where (θ_i, ϕ_i) are the polar and azimuthal angles of orientation of the axis of symmetry of the ith molecule.

The potential energy functions were then expanded in spherical harmonics, to allow analytic evaluation of the angular integrals in the λ-expansion of the free energy

$$-\beta\Delta A = \sum_{n=1}^{\infty} (-\beta\lambda)^n a_n$$

By writing

$$u_{ij}(r,\omega_i,\omega_j) = 4\pi \sum_{\ell_1\ell_2} \sum_{m} \sum \chi^{\ell_1\ell_2 m}(r) S^{m_1}_{\ell_1}(\omega_1) S^{m_1}_{\ell_2}(\omega_1) S^{m_2}_{\ell_2}(\omega_2)$$

where $\omega_i \equiv (\theta_i,\phi_i)$, and $S^{m_i}_{\ell_i}(\omega_i)$ are the spherical harmonics, the spatial and angular variables of the potential energy can be separated. Using the orthogonality properties of the spherical harmonics, and the previously derived potential energy functions we have found the following expansion coefficients for the higher order multipole interactions (ℓ_1 = 1, 2, 3, and 4 correspond to dipole, quadrupole, octopole and hexadecapole moments)

$$\chi^{131} = \chi^{130}\sqrt{3/8} = \mu_1\Omega_2\sqrt{2}/\sqrt{7}\, r^5$$

$$\chi^{232} = \chi^{231}/\sqrt{10} = \chi^{230}/\sqrt{20} = \Theta_1\Omega_2/\sqrt{7}\, r^6$$

$$\chi^{333} = \chi^{332}/6 = \chi^{331}/15 = \chi^{330}/20 = \Omega_1\Omega_2/7\, r^7$$

$$\chi^{141} = \chi^{140}\sqrt{2/5} = \mu_1\Phi_2\, 2\sqrt{5}/3\sqrt{6}\, r^6$$

$$\chi^{242} = \chi^{241}/2\sqrt{2} = \chi^{240}/\sqrt{15} = \Theta_1\Phi_2\sqrt{3}/3\, r^7$$

$$\chi^{343} = \chi^{342}/\sqrt{21} = \chi^{341}/\sqrt{105} = \chi^{340}/\sqrt{175} = \Omega_1\Phi_2/3\, r^8$$

$$\chi^{444} = \chi^{443}/8 = \chi^{442}/28 = \chi^{441}/56 = \chi^{440}/70 = \Phi_1\Phi_2/9\, r^9$$

The general pattern of these coefficients allows a check on the tedious and mistake-prone calculations.

With these results the terms of $O(\lambda^2)$ in the free energy expansion can be calculated. To go beyond this, using a Padé approximant for the free energy in the manner proposed by Stell, Rasaiah and Narang,[1] requires at least the term of $O(\lambda^3)$. To this end the corresponding angularly averaged three-body potentials for higher multipoles were needed. They were not available in the literature but were derived in the manner of R. J. Bell[3] and Rasaiah and Stell.[4]

Using quantum-mechanical perturbation theory Bell has shown that the non-additive three-body potential due to fluctuating dipoles and multipoles may be expressed as a function of the intermolecular distances and the interior angles of the triangle which they form

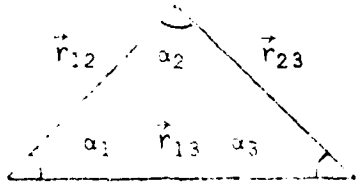

Rasaiah and Stell recognized that the corresponding three-body term in the perturbation theory of polar fluids had the same form

$$U_{123}^{eff} = Z^{\ell_1\ell_2\ell_3} W_{\ell_1\ell_2\ell_3}(r_{12},r_{13},r_{23},\alpha_1,\alpha_2,\alpha_3)$$

where $Z^{\ell_1\ell_2\ell_3}$ is a coefficient determined by ℓ_1, ℓ_2 and ℓ_3. Bell derived the geometrical factor $W_{\ell_1\ell_2\ell_3}(r_{12},r_{13},r_{23},\alpha_1,\alpha_2,\alpha_3)$ for dipoles, quadrupoles and all triplet combinations of them. On extending his work to include octopoles and hexadecapoles, we find

$$W^{113} = 5/16\, r_{12}^{-3}r_{13}^{-5}r_{23}^{-5}\{29+3\cos(\alpha_1-\alpha_2)[7\cos3\alpha_3+9\cos\alpha_3] + \cos2\alpha_3[4-49\cos2\alpha_3]\}$$

$$W^{133} = 35/256\, r_{12}^{-5}r_{13}^{-5}r_{23}^{-7}\{5[9-15\cos2\alpha_1-14\cos\alpha_1\cos3\alpha_1] + 21[22\cos\alpha_1\cos3(\alpha_2-\alpha_3)-5(\cos2(\alpha_1-\alpha_2) + \cos2(\alpha_1-\alpha_3)-18\cos2\alpha_1\cos2(\alpha_2-\alpha_3)+6\cos2(\alpha_2-\alpha_3)]\}$$

$$W^{223} = 75/256\ r_{12}^{-5}r_{13}^{-6}r_{23}^{-6}\{265\cos2\alpha_3\cos3\alpha_3-147\cos\alpha_3\cos2\alpha_3$$

$$-17\cos\alpha_3+14\cos(\alpha_1-\alpha_2)\ [5-21\cos4\alpha_3]$$

$$+49\cos2(\alpha_1-\alpha_2)\ [3\cos3\alpha_3+5\cos\alpha_3]\}$$

$$W^{233} = 35/1024\ r_{12}^{-6}r_{13}^{-6}r_{23}^{-7}\{1305\cos\alpha_1-35\cos3\alpha_1\ [29+54\cos2\alpha_1]$$

$$+42[5\cos(\alpha_1-\alpha_3)(6-11\cos2\alpha_1+21\cos4\alpha_1)$$

$$+3\cos2(\alpha_2-\alpha_3)(13\cos\alpha_1-45\cos3\alpha_1)$$

$$+11\cos3(\alpha_2-\alpha_3)(7+9\cos2\alpha_1)]\}$$

$$W^{333} = 105/1024\ r_{12}^{-7}r_{13}^{-7}r_{23}^{-7}\{2600+42\ [55\cos\alpha_1\cos\alpha_2\cos\alpha_3$$

$$-24\cos2\alpha_1\cos2\alpha_2\cos2\alpha_3+121\cos3\alpha_1\cos3\alpha_2\cos3\alpha_3]$$

$$+441\ [8(\cos2(\alpha_1-\alpha_2)+\cos2(\alpha_2-\alpha_3)+\cos2(\alpha_1-\alpha_3))$$

$$+5(\cos(\alpha_1-\alpha_2)\cos3\alpha_3+\cos(\alpha_2-\alpha_3)\cos3\alpha_1$$

$$+\cos(\alpha_1-\alpha_3)\cos3\alpha_2)+11(\cos\alpha_1\cos3(\alpha_2-\alpha_3)$$

$$+\cos\alpha_2\cos3(\alpha_1-\alpha_3)+\cos\alpha_3\cos3(\alpha_1-\alpha_2))]\}$$

$$W^{114} = 15/256\ r_{12}^{-3}r_{13}^{-6}r_{23}^{-6}\{-189\cos5\alpha_3+7\cos3\alpha_3+54\cos\alpha_3$$

$$+6\cos(\alpha_1-\alpha_2)\ [15+21\cos\alpha_3+28\cos2\alpha_3]\}$$

$$W^{144} = 105/16384\ r_{12}^{-6}r_{13}^{-6}r_{23}^{-9}\ \{105[9\cos5\alpha_1+73\cos3\alpha_1-12\cos\alpha_1]$$

$$+1080\cos(\alpha_2-\alpha_3)[6-13\cos2\alpha_1-7\cos4\alpha_1]$$

$$+1188\cos2(\alpha_2-\alpha_3)[15\cos3\alpha_1-\cos\alpha_1]$$

$$+10296\cos3(\alpha_2-\alpha_3)[1-3\cos2\alpha_1]+38610\cos\alpha_1\cos4(\alpha_2-\alpha_3)\}$$

$$W^{224} = 105/4096\ r_{12}^{-5}r_{13}^{-7}r_{23}^{-7}\ \{600+3267\cos6\alpha_3-1728\cos4\alpha_3+165\cos2\alpha_3$$

$$+20\cos(\alpha_1-\alpha_2)[110\cos\alpha_3-69\cos3\alpha_3-297\cos5\alpha_3]$$

$$+70\cos2(\alpha_1-\alpha_2)[33\cos4\alpha_3+60\cos2\alpha_3+35]\}$$

The geometric terms W^{244}, W^{334}, W^{344}, and W^{444} have yet to be obtained. Work on this is proceeding.

To determine the specific coefficient $Z^{\ell_1\ell_2\ell_3}$ in the three-body potential we made use of the spherical harmonic expansion coefficients and the method outlined by Rasaiah and Stell[4] to obtain

$$Z^{113} = \mu^4\Omega^2/63, \quad Z^{133} = \mu^2\Omega^4/147, \quad Z^{223} = \Theta^4\Omega^2/175$$

$$Z^{233} = \Omega^4\Theta^2/245, \quad Z^{333} = \Omega^6/343$$

$$Z^{114} = \mu^4\Phi^2/81, \quad Z^{144} = \mu^2\Phi^4/243, \quad Z^{224} = \Theta^4\mu^2/225$$

From these sequences one may predict the values of $Z^{\ell_1\ell_2\ell_3}$ even when the geometric terms beyond W_{224} have not yet been obtained. We expect that

$$Z^{244} = \Theta^2\Phi^4/105, \quad Z^{234} = \Omega^4\Phi^2/441$$

$$Z^{344} = \Omega^2\Phi^4/567, \quad Z^{444} = \Phi^6/729$$

To complete this portion of the work we needed to evaluate the remaining four geometric factors to obtain the effective angularly-averaged three-body potentials which contribute to the term of $O(\lambda^3)$ for all binary mixtures with multipole moments through the hexadecapole moment. The integrals of the form

$$\int g^{o}_{12}(r) u_{12}(r_{12},\omega_1,\omega_2) d\omega_1 d\omega_2 d\vec{r}_{12}$$

and

$$\int g^{o}_{123}(r_{12},r_{13},r_{23}) u^{eff}_{123}(r_{12}r_{13}r_{23})\ d\vec{r}_{12} d\vec{r}_{13} d\vec{r}_{23}$$

were then numerically evaluated using a method previously developed by Rasaiah, Larsen and Stell.[5] The result is the first and second terms for the lambda expansion from which a Padé approximant for the free energy can be formed.

In order to extend these perturbation methods to systems with non-spherical cores we must first properly characterize the reference system. To that end, we proceeded with a computer simulation of linear non-spherical molecules. The objective was to compute an ensemble averaged angularly dependent distribution function in terms of the coefficients in a spherical harmonic expansion of the distribution function

$$g(r_{12},\omega_1,\omega_2) = \sum_{\ell_1 \ell_2 m} \sum \sum g_{\ell_1 \ell_2 m}(r) S_{\ell_1}^{\ \ m}(\omega_1)\ S_{\ell_2}^{\ \ m}(\omega_2)$$

From these coefficients one may obtain, by the orthogonality of the spherical harmonics in the expansions of the distribution and potential functions, a very simple expression for the term of $O(\lambda)$ for a linear molecule with a quadrupole-moment

$$\frac{\beta\lambda a_1}{N} = \frac{4\pi\rho^{*}Q^2}{5kT\sigma^5} \int_0^{\infty} [3g_{220}(r) - 4g_{221}(r) + g_{222}(r)] \frac{dr}{r^3}$$

where σ is the diameter of one of the atoms in the diatomic molecule and ρ^* is the reduced density.

Monte Carlo simulations of the equilibrium properties of a nomonuclear diatomic molecule with molecular dimensions characteristic of Cl_2 were performed to generate an accurate set of coefficients $g_{l_1 l_2 m}(r)$ appearing in the spherical harmonic expansion of the radial distribtuion function $g(r, \omega_1, \omega_2)$. Nearly a million configurations were generated in calculating the results depicted in Fig. 1. The moments,

$$\int_0^\infty g_{l_1 l_2 m}(r) r^{-2} dr$$

which appear in the term of $O(\lambda)$ in the free energy decreased steadily by only 2.5 over the last 600K configurations. These calculations are probably more accurate than earlier determinations[6] of $g_{l_1 l_2 m}(r)$, even though the programs used were essentially the same. This is primarily because a larger number of configurations, with more frequent samplings at smaller intervals, were generated. In Table I, the newer estimates of the term of $O(\lambda)$ are compared with older data, for reduced quadrupole moments corresponding the critical point and melting point of Cl_2 at a reduced density of 0.5.

Table I

Comparison of the term of $O(\lambda)$ obtained by numerical integration of (7) using the data for $g_{220}(r)$, $g_{221}(r)$, and $g_{222}(r)$ from the independent studies of Street and Tildesley (S&T) and Eggebrecht and Rasaiah (E&R)

	Simpson's rule		Trapezoidal rule	
ρ^*	S&T	E&R	E&R	S&T
.812	.283	.328	.373	.414
1.4[illegible]	.493	.571	.652	.723
1.975	.686	.798	.907	1.006

A number of difficulties became apparent from the discrepancies in the table. The sources of error in this calculation were found to be: 1) the large fluctuations in the moments of $g_{222}(r)$; 2) the sensitivity of the function to the method of integration. The greater similarities in our estimates of the integral may be attributed to the smaller increments used in our version for the radial distance.

II. Adsorption of Dipoles and Ions at a Wall in the Presence of an Electric Field

While our understanding of the behavior of liquids has improved dramatically over the past ten years, the physics and chemistry of surface phenomena is still at a primitive stage. One of the outstanding problems in this area is the elucidation of the density profiles of ions and dipoles at a charged surface; a detailed knowledge of this is fundamental to our understanding of phenomena ranging from the behavior of electrodes in batteries to selective adsorption and transport across membranes. It is convenient to study ions and dipoles at a surface separately before trying to gain insight into the behavior of a mixture of these two. We have, therefore, embarked upon a program in which the following problems will be studies in sequence.

1) Dipoles at a wall in the presence of an electric field.

2) Ions at a charged interface.

3) Dipoles and charges at a wall in the presence of an electric field.

Investigation of the first problem has progressed very rapidly in collaboration with Dr. Dennis Isbister and John Eggebrecht. Professor Noel Thompson, a visitor on sabbatical leave from Australia, Dr. Dennis Isbister,

and I have made progress on the second problem, while work on mixtures of ions and dipoles at a wall has only just begun. In what follows, we provide a brief description of our work on dipoles at a wall.

The effect of a wall is obtained by allowing a mixed system of at least two species 1 and 2 to change in such a way that the density of one species (2 say) goes to zero accompanied by an increased in diameter R_2. It is the growth of this single particle (2) that emerges finally as a wall, and if the wall-particle had a dipole-moment, the zero density - infinite radius limit could be made to produce an electric field as well emerging at any chosen angle from the wall. The density profile ρ_1 of each fluid species near the wall is given by

$$\rho_1(r) = \lim_{R_2\to\infty} \lim_{\rho_2\to 0} \rho_1^{o}[h_{21}(\rho,\Omega_1,\Omega_2)+1]$$

where ρ_1^{o} is the bulk density of species 1, and $h_{21}(r)$ is total wall-particle correlation function which has the usual invariant expansion.

Our initial investigation of dipoles at a wall used the linearized hypernetted chain (LHNC) closure for the wall-particle and particle-particle interactions.

It is known that this approximation leads to fairly accurately bulk properties for dipoles. We found that the contact values for the wall-particle correlation function are much higher than those obtained in the mean spherical (MS) approximation.[7]

The linearized hypernetted chain closure is obtained by taking the first term in the expansion of the angular part of $\ln(h_{21}+1)$ which appears in the hypernetted chain (HNC) approximation for the direct correlation function C_{21}. If the second term is retained as well, a more accurate

description of the system results. This approximation, known as the quadratic hypernetted chain, QHNC,[8,9] reveals a new phenomenon that is absent in the MS and LHNC approximations. This is the change in the density of the fluid in an open system when the electric field is turned on, and is called electrostriction. The leading term in the relative change in density K_h at an infinite distance from the wall was found, in the QHNC approximation, to be given by a term of $O(E^2)$

$$k_h^{(2)} = \frac{\Delta\rho}{\rho_1^{\circ}} = \frac{\beta}{24\pi\rho_1^{\circ}y}(\varepsilon-1)^2\frac{E^2}{Q}$$

where E is the electric field, Q the inverse compressibility, ε the dielectric constant, and $y = \frac{4\pi}{9} m_1^2 \rho_1^{\circ} \beta$, with $\beta = 1/kT$. Approximations beyond the QHNC theory systematically generate term of higher order, so that this approximation must contain the complete electrostriction term of $O(E^2)$ in the HNC approximation. However, a discrepancy in K_h was found on comparing our result with the thermodynamics of electrostriction in an open system.[10] Since the HNC approximation and all of the theories derived from it ignore bridge diagrams, the discrepancy in the term of $O(E^2)$ between the QHNC result and thermodynamics must come from neglect of these diagrams. The lowest order bridge diagram was then calculated and found to contribute significantly to electrostriction. Adding this to the QHNC result of $O(E^2)$, we obtained (resolving the above discrepancy)

$$K_h \simeq \left[\frac{\beta(\varepsilon-1)^2}{24\pi\rho_1^{\circ}y} - \frac{5(\varepsilon-1)^2\beta y}{128\pi\rho_1^{\circ}}\right]\frac{E^2}{Q}$$

which shows that the bridge diagrams cannot be ignored in calculations of the local density at an infinite distance away from the wall. It appears likely that they affect the density profiles also when the dipoles are

closer to the wall. This is an important result, because all of the theoretical studies of the ordering of dipoles and ions at a wall that have been carried out so far ignore these bridge diagrams.

Our study of the LHNC approximation for the wall-particle distribution function leads to the constitutive relation

$$\vec{P}(\infty) = (\varepsilon-1)\ \vec{E}(\infty)/4\pi$$

between the polarization denisty $\vec{P}(\infty)$ and the electric field $\vec{E}$ with the same dielectric constant ε as that obtained in relating ε to the two-particle correlation function of a dipolar fluid in the absence of an electric field. The QHNC approximation, however, yields in addition non-linear terms in the electric field for the polarization density. We plan to extend this work to mixtures of dipoles in order to study the selective adsorption of dipoles near an electrified wall.

References

1. G. Stell, J. C. Rasaiah and H. Narang, Molec. Phys., 27, 1393 (1974).
2. S. Kielich in Specialist Periodic reports on Dielectric and Related Molecular Processes, Vol. 1, Chemical Society, Lond. 1972.
3. R. J. Bell, J. Phys., B3, 751 (1970).
4. J. C. Rasaiah and G. Stell, Chem. Phys. Lett., 25, 519 (1974).
5. (a) J. C. Rasaiah, B. Larsen and G. Stell, J. Chem. Phys., 63, 722 (1975).
   (b) B. Larsen, J. C. Rasaiah and G. Stell, Mol. Phys., 33. 987 (1977).
6. W. B. Street and D. Tildesley, J. Chem. Phys., 68, 1275 (1978).
7. J. M. Eggebrecht, D. J. Isbister and J. C. Rasaiah, J. Chem. Phys., 73, 3980 (1980).
8. J. C. Rasaiah, D. J. Isbister and G. Stell, Chem. Phys. Lett., 79, 189 (1981).
9. J. C. Rasaiah, D. J. Isbister and G. Stell, J. Chem. Phys., (1981) to appear.
10. J. G. Kirkwood and J. Oppenheim, Chap. 14, Chemical Thermodynamics (McGraw Hill, New York, 1961).

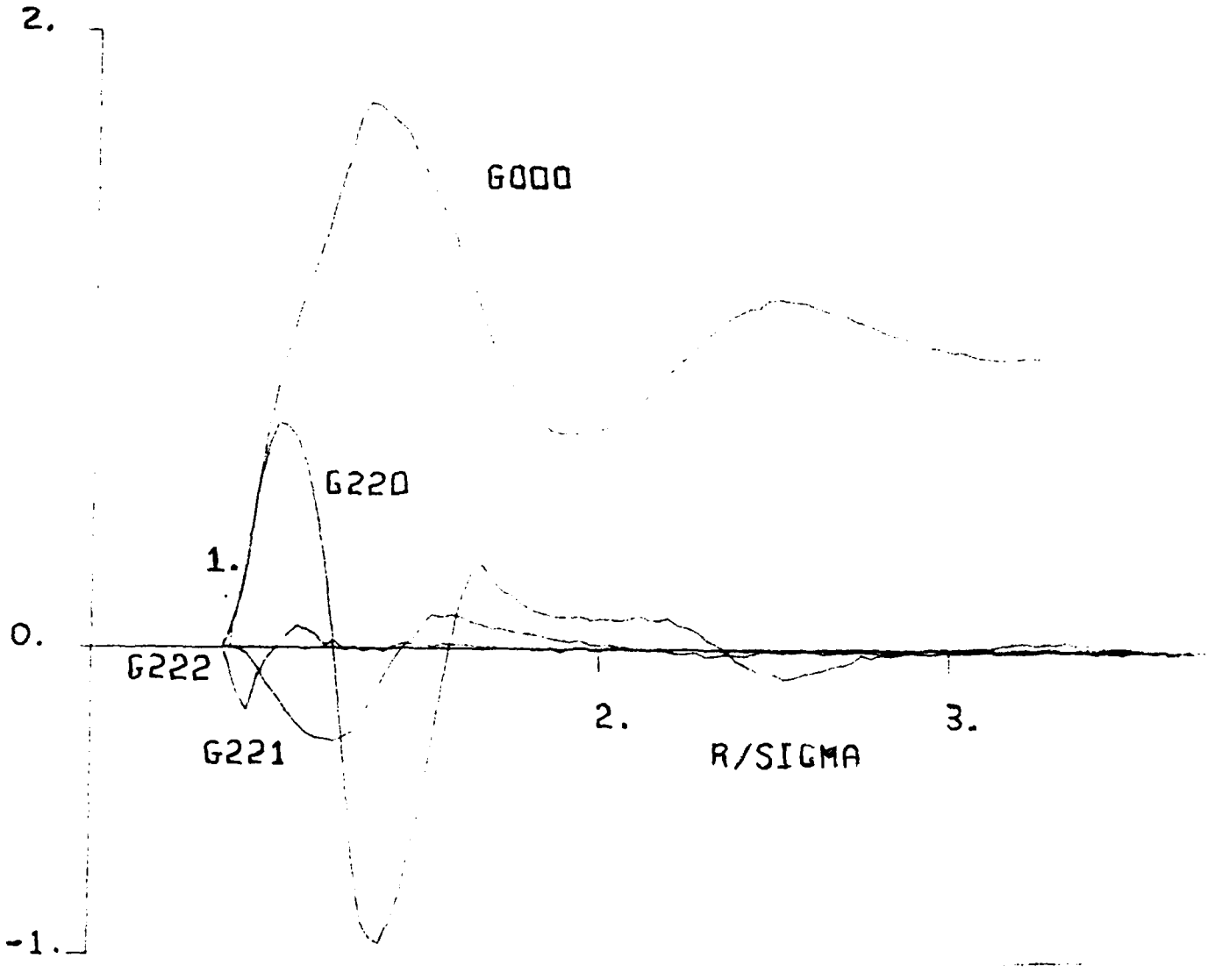

Fig.1 The coefficients of the spherical harmonic expansion of the angle dependant distribution function after two million configurations.

ELECTROSTRICTION AND DIPOLAR ORDERING AT AN ELECTRIFIED WALL

J.C. RASAIAH
Department of Chemistry, University of Maine, Orono, Maine 04469, USA

D.J. ISBISTER
Department of Chemistry, University of New South Wales, Duntroon, ACT 2600, Australia

and

G. STELL
Departments of Mechanical Engineering and Chemistry, State University of New York, Stony Brook, New York 11794, USA

Received 22 January 1981; in final form 3 March 1981

A theory of electrostriction which follows from studies of dipolar ordering at an electrified wall is discussed in the quadratic hypernetted chain approximation. Bridge diagrams for the wall - particle correlation functions contribute significantly to electrostriction even to lowest order in the electric field. The form of the constitutive relation between the polarization density and the field in strong fields is discussed.

1. Introduction

The ordering of dipoles at a wall from which an electric field emerges has been studied in the mean spherical (MS) [1] and linearized hypernetted chain (LHNC) [2] approximations. We report here that electrostriction appears as an added feature when the theory is carried beyond the LHNC approximation for the wall - particle correlation functions, leading to a molecular theory of this phenomenon in which graphical analysis and integral equation approximations that are ubiquitous in the theory of fluids may be exploited. Of the hierarchy of approximations generated by the hypernetted chain equation (HNC), we find that the quadratic hypernetted chain (QHNC) approximation is the first to predict electrostriction. The leading term in the relative change in density an *infinite distance* away from a flat wall is of $O(E^2)$, where E is the magnitude of the local field. Approximations beyond the QHNC theory systematically generate terms of higher order, so that the QHNC approximation also contains within it the complete electrostriction term of $O(E^2)$ in the HNC approximation.

All of the theories of electrostriction which have their genesis in the HNC approximation ignore the bridge diagrams, but we find, by comparing the QHNC theory with the thermodynamics of electrostriction [3], that these diagrams must contribute significantly even to lowest order in E. This leads us to believe that they play an equally important role in determining the local density when the dipoles are closer to the wall.

We report here the barest outline of our molecular theory for an open system [4] in which contributions from the QHNC approximation to $O(E^2)$ and from the bridge diagrams to the same order in the electric field and to lowest order in the density and the dipole moment are evaluated analytically. Our theory can also be extended to higher order in E but this will not be pursued here. The thermodynamic discussion of Kirkwood and Oppenheim [3] however is limited to deriving the electrostriction term of $O(E^2)$, since it is based on a thermodynamic perturbation theory of first order in E^2, that uses as reference-state input the linear constitutive relation between the polarization density $P(\infty)$ and the local electric field E for a field-independent ϵ,

$$P(\infty) = (\epsilon - 1)\, E(\infty)/4\pi. \quad (1)$$

Further details of our work and extensions to it will be presented elsewhere [4] but we remark that our study yields the constitutive relation with the same value of ϵ as that obtained from from relating ϵ to the two-particle orientational correlation function in the absence of a field, and also provides a basis for determining non-linear terms in the electric field for the polarization density.

2. Electrostriction in an open system

We employ the technique discussed in refs. [1,2] to generate an electric field by taking a mixture of dipolar hard spheres to the zero-density limit of species 2 with an attendant increase in the radius R_2 to infinity, under the constraint that its dipole moment m_2 divided by the cube of the radius of the excluded volume $R_{21} = R_2 + R_1$ is a constant E_0. The electric field E_2 emerging from the wall is related to E_0 by [1,2]

$$E_2 = E_0 (3\cos^2\theta_2 + 1)^{1/2}\, e_2, \quad (2)$$

where e_2 is a unit vector dependent upon θ_2 [1,2], the angle which the wall dipole makes with the wall normal n. Note that E_2 is constant when the wall dipole orientation θ_2 is fixed. The relationship between E_2 and the Maxwell field E in the fluid is of the form

$$E = [3/(2\epsilon + 1)]\, E_2 + \text{terms non-linear in } E_2. \quad (3)$$

Here the non-linear terms are of magnitude const. $E_2^3 + \ldots$ when $\theta_2 = 0$, and ϵ is the dielectric constant of the fluid at zero field. In the notation of ref. [2], the wall–particle correlation function has the invariant expansion

$$h_{21}(z, E_2, \boldsymbol{\Omega}_1) = h_{21}^{s}(z) + h_{21}^{D}(z)\, D(2,1) + h_{21}^{\Delta}(z)\, \Delta(2,1) + \ldots, \quad (4)$$

where $\Delta(2,1) = \hat{s}_2 \cdot \hat{s}_1$ and $D(2,1) = \hat{s}_2 \cdot (3\hat{n}\hat{n} - \mathbf{U}) \cdot \hat{s}_1$ in which $\hat{s}_2$ and $\hat{s}_1$ are unit vectors in the directions of the wall dipole and fluid dipole respectively, z is the distance of a fluid dipole (of orientation $\boldsymbol{\Omega}_1$) from the wall, and $\mathbf{U}$ is the unit tensor. In this wall limit, $R_2 \to \infty$,

$$h_{21}^{D}(z) = \dot{h}_{21}^{D}(z) + 3K_{21}, \quad (5)$$

where $\dot{h}_{21}^{D}(z)$ is short-ranged and K_{21} is a constant related to the electric field E_2 (see section 3). Hence

$$\lim_{z\to\infty} h_{21}^{D}(z) = 3K_{21} \quad (6)$$

The origin of electrostriction in our theory is the coupling that can exist between $h_{21}^{D}(z)$ and $h_{21}^{s}(z)$; this feedback begins with the QHNC approximation.

We define the electrostriction effect K_h as the relative change in density of the bulk fluid when the electric field is switched on, so that

$$K_h \equiv \Delta\rho/\rho_1^0 = h_{21}^{*}(\infty, E_2). \quad (7)$$

where

$$h_{21}^{*}(z, E_2) = \Omega^{-1} \int h_{21}(z, E_2, \boldsymbol{\Omega}_1)\, \mathrm{d}\boldsymbol{\Omega}_1. \quad (8)$$

$\Omega = 4\pi$ for dipolar hard spheres and ρ_1^0 is the density of the bulk fluid when $E_2 = 0$. If K_c is the corresponding asymptotic limit of the angularly averaged direct correlation function $c_{21}(z, E_2, \boldsymbol{\Omega}_1)$, we find [4] that, in the absence of molecular polarizability

$$K_h = K_c\, Q. \quad (9)$$

where Q is the inverse compressibility of the fluid,

$$Q = 1 - (\rho_1^0/\Omega^2) \int c_{11}(r, \boldsymbol{\Omega}_1, \boldsymbol{\Omega}_3)\, \mathrm{d}\boldsymbol{\Omega}_1\, \mathrm{d}\boldsymbol{\Omega}_3\, \mathrm{d}r \quad (10)$$

and $c_{11}(r, \boldsymbol{\Omega}_1, \boldsymbol{\Omega}_3)$ is the direct correlation function of the bulk fluid. The thermodynamic theory of electrostriction [3] for an open system gives K_h to $O(E^2)$ as

$$K_h^{(2)} = (\beta/8\pi)\, (\partial\epsilon/\partial\rho_1^0)\, E^2\, Q. \quad (11)$$

where $\beta = 1/kT$, k is Boltzmann's constant, T is the absolute temperature and the superscript (2) means the term of $O(E^2)$.

3. The QHNC approximation for electrostriction

By considering the asymptotic limit of $c_{21}^{D}(z)$ in the invariant expansion for the wall–particle direct correlation function $c_{21}(z, E_2, \boldsymbol{\Omega}_1)$ we find [4] that K_{21} is related to E_2 in the QHNC approximation by

$$\beta m_1 E_2/(3\cos^2\theta_2+1)^{1/2} = K_{21}[2Q_+(2K_{11}\rho_1^0 R_{11}^3) + Q_-(-K_{11}\rho_1^0 R_{11}^3) - 3K_h/(1+K_h)], \quad (12)$$

where the $Q_\pm(\ )$ functions are defined in ref. [2], and the constant K_{11} is related quite generally (i.e. not just in the QHNC theory) to the fluid dipole moment m_1 by [4–6]

$$3y = Q_+(2K_{11}\rho_1^0 R_{11}^3) - Q_-(-K_{11}\rho_1^0 R_{11}^3), \quad (13)$$

where $y = 4\pi m_1^2 \rho_1^0 \beta/9$. The dielectric constant ϵ of the fluid is also quite generally given by [6]

$$\epsilon = Q_+(2K_{11}\rho_1^0 R_{11}^3)/Q_-(-K_{11}\rho_1^0 R_{11}^3). \quad (14)$$

We also find from the $z \to \infty$ limit of the QHNC approximation for $c_{21}(z, E_2, \mathbf{\Omega}_1)$ that

$$K_c^{(2)} = \tfrac{3}{2} K_{21}^2 (3\cos^2\theta_2 + 1) \quad (15)$$

and on using (2), (3), (9) and (12) – (14) we have

$$K_h^{(2)} = (\beta/24\pi\rho_1^0 y)(\epsilon - 1)^2 E^2/Q, \quad (16)$$

where the superscript (2) means again the term of $O(E^2)$. Note that in (16) $K_h^{(2)}$ is independent of the inclination θ_2 of the wall dipole. Consistency with the thermodynamic theory (11) demands that

$$\rho_1^0 \partial\epsilon/\partial\rho_1^0 = (\epsilon - 1)^2/3y. \quad (17)$$

This relation is indeed satisfied by the simple Debye equation $(\epsilon - 1)/(\epsilon + 2) = y$, but the more exact expression [7,8] (for arbitrary y and $\rho_1^0 \to 0$)

$$(\epsilon - 1)(\epsilon + 2) = y - \tfrac{15}{16} y^3 + \ldots \quad (18)$$

introduces a discrepancy of $O(y^2)$ in (17). Since higher order approximations derived from the HNC equation do not produce additional contributions to K_h of $O(E^2)$, the apparent inconsistency lies in ignoring the bridge diagrams.

4. Bridge diagrams of $O(E^2)$

The bridge diagram of $O(E^2)$ and to lowest order in the fluid density can be represented graphically, when $z \to \infty$, by

$B^*(2,1) =$  , (19)

where 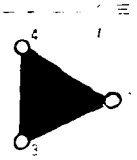 $\equiv 3K_{21} D(2,i)$, and

is the three-particle direct correlation function $c_3(X_1, X_3, X_4)$ for the fluid with $X_i \equiv (r_i, \mathbf{\Omega}_i)$. $B^*(2,1)$ contributes to the wall-particle direct correlation function. In (19) the open circle 2 is the wall dipole root point, the half black circle ◗ signifies angular integration over the orientations of the bulk fluid dipole 1 and the black circles (field points) represent spatial and angular integrations of fluid dipoles. To evaluate (19) to lowest order in ρ_1^0 and m_1 we use the low-density limit in terms of Mayer f functions

$$c_3(X_1, X_3, X_4) \sim f(X_1, X_3)\, f(X_3, X_4)\, f(X_4, X_1) \quad (20)$$

and retain only the $n = 1$ term in the perturbation expansion [8,9]

$$f(X_i, X_j) = f_0(r_{ij}) + [1 + f_0(r_{ij})] \sum_{n=1}^{\infty} [\beta m_1^2 D(i,j)/r_{ij}^3]^n / n! \quad (21)$$

for the Mayer f function, where $f_0(r_{ij})$ is the corresponding Mayer function for the reference hard-sphere system. The bridge diagram is now evaluated analytically using Hankel transforms and we find eventually that when $z \to \infty$,

$$B^{(2)*}(\infty) \simeq -\tfrac{5}{128}(\epsilon - 1)^2 \beta y E^2 \pi\rho_1^0, \quad (22)$$

in which the contribution from the three-particle correlation function appears as the third virial coefficient for hard spheres! Adding this to (16), after using (9), we have

$$K_h^{(2)} \simeq \left[\frac{\beta(\epsilon-1)^2}{24\pi\rho_1^0 y} - \frac{5(\epsilon-1)^2\beta y}{128\pi\rho_1^0}\right]\frac{E^2}{Q}, \quad (23)$$

where $\simeq$ emphasizes that our calculation of the bridge diagram of $O(E^2)$ is correct only to lowest order in ρ_1^0 and m_1. This is sufficient however to test the molecular theory against thermodynamics using (18) for the dielectric constant. Instead of (17) we now need

$$\rho_1^0 \partial\epsilon/\partial\rho_1^0 \sim (\epsilon - 1)^2/3y - \tfrac{5}{16}(\epsilon - 1)^2 y, \quad (24)$$

which is consistent with (18) to $O(y^2)$. We have thus

shown that the bridge diagrams make significant contributions to the density when $z \to \infty$, and it appears likely that they affect the density profiles also when the dipoles are closer to the wall. Theoretical studies of the ordering of dipoles and ions at a wall that have appeared so far ignore these bridge diagrams.

5. The polarization density $P(\infty, E_2)$ in an open system

From the definition of $P(z, E_2)$ in the grand ensemble [6] we have

$$P(z, E_2) = (m_1 \rho_1^0 \Omega) \int h_{21}(z, E_2, \Omega_1) s_1(\Omega_1) \, d\Omega. \quad (25)$$

In our discussion E_2 is independent of z [see (2)]. Using the invariant expansion for $h_{21}(z, E_2, \Omega_1)$, we find, after doing the necessary angular integrations, that

$$P(\infty, E_2) = m_1 \rho_1^0 K_{21} (3 \cos^2\theta_2 + 1)^{1/2} \hat{e}_2, \quad (26)$$

which is independent of any approximation for the wall–particle correlation function! Employing the QHNC approximation for K_{21} given in (12),

$$P(\infty, E_2) = \beta \rho_1^0 m_1^2 E_2 [2Q + (2K_{11}\rho_1^0 R_{11}^3) + Q \{ -K_{11}\rho_1^0 R_{11}^3) - 3K_h/(1 + K_h)\}]^{-1} \quad (27)$$

$$= [(\epsilon - 1)/4\pi][3E_2/(2\epsilon + 1)] \times \left[1 - \frac{K_h}{Q(1 + K_h)} \frac{\epsilon - 1}{2\epsilon + 1}\right]^{-1}. \quad (28)$$

When $K_h = 0$ (i.e. in the absence of electrostriction as in the MS and LHNC approximation) and when all the higher coefficients of E_2^n ($n \geq 3$) in (3) are assumed zero, we recover the constitutive relation (1). Conversely when K_h and the higher coefficients in (3) are not zero, non-linear terms in the polarization density will appear. Substitution of (15) and (9) in (28) followed by expansion of the denominator draws out the term of $O(E_2^3)$ in the QHNC approximation for the polarization density which is

$$P_{\mathrm{QHNC}}(\infty, E) = [(\epsilon - 1)/4\pi][3E_2/(2\epsilon + 1)] \times \left[1 + \frac{3\beta}{8\pi\rho_1^0 V^2} \left(\frac{\epsilon - 1}{2\epsilon + 1}\right)^3 \frac{E_2^2}{Q}\right] + O(E_2^5). \quad (29)$$

If the non-linear terms in (3) are neglected

$$P_{\mathrm{QHNC}}(\infty, E) = [(\epsilon - 1)/4\pi]E \times \left[1 + \frac{\beta}{24\pi\rho_1^0 V^2} \frac{(\epsilon - 1)^3}{2\epsilon + 1} \frac{I^2}{Q}\right] + O(I^5). \quad (30)$$

A more complete calculation of this term in the QHNC approximation would require the determination of the coefficient of the E_2^3 term in (3) when $\theta_2 = 0$. An exact calculation of the term of $O(I^3)$ would require in addition that the contributions of the bridge diagrams to electrostriction [see (22)] and to the relationship between K_{21} and I_2 be included.

Acknowledgement

JCR acknowledges support from the National Science Foundation Contract No. CHE 77-10023 and the Office of Naval Research Contract No. N0014 78-C-0724, and thanks Professors Barry Ninham and Richard Bearman for their hospitality in Australia where most of this work was done. DJI acknowledges support from the Australian Research Grants Commission. Acknowledgement is made by GS to the National Science Foundation, and to the Donors of the Petroleum Research Fund, administered by the American Chemical Society, for support of his research.

References

[1] D.J. Isbister and B.C. Treasler, J. Stat. Phys. 20 (1979) 331.
[2] J.M. Eggebrecht, D.J. Isbister and J.C. Rasaiah, J. Chem. Phys. 73 (1980) 3980.
[3] J.G. Kirkwood and I. Oppenheim, Chemical thermodynamics (McGraw-Hill, New York, 1961) ch. 14.
[4] J.C. Rasaiah, D.J. Isbister and G. Stell, to be published.
[5] C.J.F. Bottcher, Theory of electric polarization, Vol. 1, 2nd Ed. (Elsevier, Amsterdam, 1973); L. Onsager, J. Am. Chem. Soc. 58 (1936) 1486.
[6] M.S. Wertheim, Ann. Rev. Phys. Chem. 30 (1979) 471.
[7] D.W. Jepsen, J. Chem. Phys. 44 (1966) 774.
[8] G.S. Rushbrooke, Mol. Phys. 37 (1979) 761.
[9] D.W. Jepsen and H.L. Friedman, J. Chem. Phys. 38 (1963) 846.

The adsorption of dipoles at a wall in the presence of an electric field: The RLHNC approximation[a)]

John M. Eggebrecht, Dennis J. Isbister,[b)] and Jayendran C. Rasaiah

Department of Chemistry, University of Maine, Orono, Maine 04469
(Received 12 May 1980; accepted 10 June 1980)

The adsorption of dipolar hard spheres in the presence of an external electric field has previously been studied within the context of the mean spherical approximation. In order to quantify the significance of the physical trends found above, the problem is solved within the higher order closure rules afforded by the linearized hypernetted chain approximation. Expressions for the reduced dipole moment and the electric field strength are derived using only the asymptotic forms of the direct correlation functions. It is found that the favorable orientational correlations between the dipolar hard spheres and the wall are underestimated by the mean spherical approximation. This is emphasized in the enhanced adsorption of the dipolar species (at the wall itself) for dipoles oriented close to the direction of the field. However, the nonphysical features of the mean spherical approximation (manifested in the negativity of the density profile) are not fully rectified by the use of the linearized hypernetted chain approximation.

I. INTRODUCTION

The adsorption of dipolar molecules at a wall, in the presence of an electric field, is of interest in the study of electrode and membrane phenomena. Here the adsorption phenomenon is delineated by the distribution of molecules at a particular orientation Ω_1 and distance z from a hard planar wall $\rho_1(z, \mathbf{E}_2, \Omega_1)$. The electric field $\mathbf{E}_2$ emanates from this wall, the declination of the field with respect to the wall being allowed by its nonconductive properties. Isbister and Freasier[1] have investigated this problem for hard dipolar spheres against a hard wall using the mean spherical approximation (MSA). Their results for the density profile $\rho_1(z, \mathbf{E}_2, \Omega_1)$ of dipoles are of great interest even though they suffer from the defect that the wall particle density profile $\rho_1(z, \mathbf{E}_2, \Omega_1)$ assumes negative values at certain relative orientations of electric field ($\mathbf{E}_2$) and dipole moment m_1 of the particles in the fluid (the dipole orientation is denoted here by Ω_1). However, the argument leading to the electric field at the wall is not swayed by the approximation used, and may be employed with more accurate theories such as, for example, the linearized hypernetted chain (LHNC) approximation. While these theories could be expected to produce better results, they do suffer from the necessity of employing numerical methods to a greater extent than is needed to determine the density profiles in the mean spherical approximation.

This paper is devoted to a study of the wall–particle density profile using the linearized hypernetted chain approximation[2] for the wall particle and particle–particle interactions, except that the effects that are independent of the orientations of the electric field and the fluid dipole are treated exactly. In our study, these are the interactions between the hard cores in the fluid, and also the interactions between these cores and the hard wall. We call this the renormalized linearized hypernetted chain approximation (RLHNC) after the nomenclature introduced by Stell and Weis.[3] Our results for this theory are an improvement over the corresponding MS approximation when the system is characterized by (a) a reduced fluid density $\rho_1^* = \rho_1 R_{11}^3$ of 0.573, (b) a reduced dipole moment $m_1^* = m_1 \sqrt{kTR_{11}^3}$ of $\sqrt{0.5}$ (or equivalently a reduced temperature $T^* \equiv 1\ m_1^{*2}$ of 2), and (c) a reduced external electric field $E_2^* = E_2 R_{11}^3\ m_1$ of 8/3. In contrast to the MS approximation, the RLHNC wall–particle density functions $\rho_1(z, \mathbf{E}_2, \Omega_1)$ are only marginally negative near the wall for a dipole orientation in direct opposition to the field (see Fig. 2). These functions, however, can become negative over a larger distance z from the wall when the reduced dipole moment is increased to 1.0 without altering the reduced electric field or reduced density (Fig. 5). This suggests even higher order terms, beyond the RLHNC approximation, must be included in the theory when the dipole moment m_1 and the external electric field E_2 are both large.

II. GENERAL THEORY

The technique of producing a wall next to a fluid by taking the limiting behavior of a binary mixture (with densities ρ_1, ρ_2 and radii R_1, R_2) detailed by

$$\lim_{R_2 \to \infty} \lim_{\rho_2 \to 0} \tag{2.1}$$

is well known.[4] Isbister and Freasier[1] have extended this to introduce an electric field, as well, by considering the corresponding limit for a dipolar mixture under the restriction that the dipole moment m_2 of particle 2, which eventually becomes the wall, divided by the cube of the radius of the excluded volume $R_{21} = R_2 - R_1$ is a constant (hereafter called E_0):

$$\lim_{R_2 \to \infty} m_2 / R_{21}^3 = E_0 \ . \tag{2.2}$$

In taking these limits, in the specific order $\rho_2 \to 0$, $R_2 \to \infty$, the volume of the system is allowed to grow faster than R_2^3, keeping ρ_1 constant through the constraint that $\rho_2 R_2^3 \to 0$.

The magnitude and direction of the electric field $\mathbf{E}_2$

[a)] Extracted in part from the M.S. (Chemistry) thesis of J. Eggebrecht, University of Maine (1980).

[b)] Present address: Department of Chemistry, Faculty of Military Studies, University of New South Wales, RMC, Duntroon, ACT 2600, Australia.

 0021 9606 80/203980 07$01.00

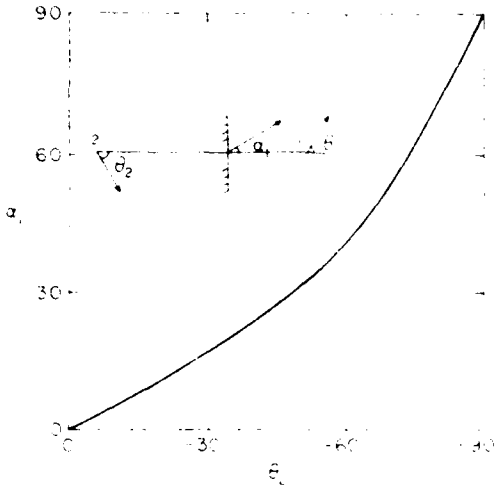

FIG. 1. The electric field angle α_1 at the wall plotted against the inclination θ_2 of the "wall dipole" which resides at minus infinity and produces the electric field E_0. The angle ξ_2 is the inclination of a dipole in the bulk fluid.

follow, when this limit is applied to the dipole–dipole interaction energy

$$V_{21}(\mathbf{r}_{21}, \Omega_2, \Omega_1) = -\frac{m_1 m_2}{r_{21}^3} D(2,1) \ , \tag{2.3}$$

Here

$$D(2,1) = \hat{s}_1 \cdot (3\hat{r}_{21}\hat{r}_{21} - \mathbf{U}) \cdot s_2 \ , \tag{2.4}$$

$\hat{s}_1$ and $\hat{s}_2$ are unit vectors in the directions of the dipole moment vectors $\mathbf{m}_1$ and $\mathbf{m}_2$, respectively. $(3\hat{r}_{21}\hat{r}_{21} - \mathbf{U})$ is the dipole–dipole interaction tensor, in which $\hat{r}_{21}$ is a unit vector in the direction along the line joining particles 1 and 2, and $\mathbf{U}$ is the unit tensor. The potential may be written in terms of the electric field $\mathbf{E}_2$, produced at the location of particle 1 by the second particle 2,

$$V_{21}(\mathbf{r}_{21}, \Omega_2, \Omega_1) = -m_1 \hat{s}_1 \cdot \mathbf{E}_2 \ , \tag{2.5}$$

where

$$\mathbf{E}_2 = \frac{m_2}{r_{21}^3} \mathbf{e}_2 \ . \tag{2.6}$$

In Eq. (2.6)

$$\mathbf{e}_2 = (3\hat{r}_{21}\hat{r}_{21} - \mathbf{U}) \cdot \hat{s}_2 = (3\hat{r}_{21}\cos\theta_2 - \hat{s}_2) \tag{2.7}$$

and θ_2 is the angle which the dipole embedded in particle 2 makes with $\hat{r}_{21}$ (see Fig. 1). Since the magnitude of $\mathbf{e}_2$ is $(3\cos^2\theta_2 + 1)^{1/2}$,

$$\mathbf{E}_2 = \frac{m_2}{r_{21}^3}(3\cos^2\theta_2 + 1)^{1/2}\hat{e}_2 \ , \tag{2.8}$$

where $\hat{e}_2$ is a unit vector in the direction of $\mathbf{E}_2$. Changing variables to $r_{21} = R_2 + z$, and taking the wall limit, the electric field

$$\mathbf{E}_2 = E_0(3\cos^2\theta_2 + 1)^{1/2}\hat{e}_2 \ , \tag{2.9}$$

which shows that $\mathbf{E}_2$ is independent of the distance z from the wall, but that its magnitude is determined by the strength (through E_0) and the direction (through θ_2) of the "wall dipole," which has receded to a distance $-z$ from the wall. At that distance, the vector $\mathbf{r}_{21}$ becomes perpendicular to the wall, and the electric field which makes an angle α_1 with respect to this normal is given by the appropriate solution to

$$\cos\alpha_1 = \hat{e}_2 \cdot \hat{r}_{21} = \frac{2\cos\theta_2}{(3\cos^2\theta_2 + 1)^{1/2}} \ . \tag{2.10}$$

The solution to this equation gives the direction of the electric field uniquely, in terms of the orientation of the wall dipole at minus infinity (see Fig. 1).

The density profile $\rho_1(z, \mathbf{E}_2, \Omega_1)$ of dipolar molecules at a distance z from the wall depends on the dipole orientation Ω_1, on the direction of the electric field $\mathbf{E}_2$ and on other parameters of the system. It is obtained from the relation[1]

$$\rho_1(z, \mathbf{E}_2, \Omega_1) = \lim_{R_2 \to \infty} \left\{ \lim_{\rho_2 \to 0} \rho_1 \, g_{21}(r_{21}, \Omega_2, \Omega_1) \right\} \ , \tag{2.11}$$

where ρ_1 is the bulk density of species 1 and $g_{21}(r_{21}, \Omega_2, \Omega_1)$ is the total correlation function of species 1 and 2 in a binary mixture. The latter is the solution to the Ornstein–Zernike relation

$$h_{21} = c_{21} + \frac{1}{4\pi}\sum_{\gamma=1}^{2} \rho_\gamma \, h_{2\gamma} * c_{\gamma 1} \ , \tag{2.12}$$

where $* = \int d\mathbf{r}_3 d\Omega_3$ is a convolution involving spatial and angular integrations. Assuming the invariant expansions

$$h_{21}(r_{21}, \Omega_2, \Omega_1) = h_{21}^{S}(r_{21}) + h_{21}^{\Delta}(r_{21})\Delta(2,1) + h_{21}^{D}(r_{21})D(2,1) \ , \tag{2.13}$$

$$c_{21}(r_{21}, \Omega_2, \Omega_1) = c_{21}^{S}(r_{21}) + c_{21}^{\Delta}(r_{21})\Delta(2,1) + c_{21}^{D}(r_{21})D(2,1) \ , \tag{2.14}$$

and using Wertheim's multiplication table[2] in Fourier space for the angular integrations, the Ornstein–Zernike relation reduces to three equations

$$h_{21}^{S} = c_{21}^{S} + \sum_{\gamma=1}^{2} \rho_\gamma \, h_{2\gamma}^{S} * c_{\gamma 1}^{S} \ , \tag{2.15}$$

$$\hat{h}_{21}^{D} = \hat{c}_{21}^{D} + \frac{1}{3}\sum_{\gamma=1}^{2} \rho_\gamma (\hat{h}_{2\gamma}^{D} * \hat{c}_{\gamma 1}^{S} + \hat{h}_{2\gamma}^{D} * c_{\gamma 1}^{\Delta} + h_{2\gamma}^{\Delta} * \hat{c}_{\gamma 1}^{D}) \ , \tag{2.16}$$

$$h_{21}^{\Delta} = c_{21}^{\Delta} + \frac{1}{3}\sum_{\gamma=1}^{2} \rho_\gamma (2\hat{h}_{2\gamma}^{D} * \hat{c}_{\gamma 1}^{D} + h_{2\gamma}^{\Delta} * c_{\gamma 1}^{\Delta}) \ , \tag{2.17}$$

when $* = \int d\mathbf{r}_3$ is a convolution involving only spatial integrations. In Eqs. (2.16) and (2.17)

$$\hat{h}_{\alpha\beta}^{D}(r) = h_{\alpha\beta}^{D}(r) - 3\int_{r}^{\infty} ds \, s^{-1} h_{\alpha\beta}^{D}(s) \tag{2.18}$$

and its inverse is

$$h_{\alpha\beta}^{D}(r) = \hat{h}_{\alpha\beta}^{D}(r) - \frac{3}{r^3}\int_{0}^{r} \hat{h}_{\alpha\beta}^{D}(s) \, s^2 ds \ , \tag{2.19}$$

with similar expressions for $\hat{c}_{\alpha\beta}^{D}(r)$ and $c_{\alpha\beta}^{D}(r)$ in which $\alpha, \beta = 1$ or 2. Inside the hard cores

$$\begin{aligned} &h_{\alpha\beta}^{S}(r) = -1 \ , \\ &h_{\alpha\beta}^{D}(r) = h_{\alpha\beta}^{\Delta}(r) = 0 \ , \quad r < R_{\alpha\beta} = R_\alpha + R_\beta \ , \end{aligned} \tag{2.20}$$

so that from Eq. (2.18)

$$\hat{h}_{\alpha\beta}^{D}(r) = -3K_{\alpha\beta} \ , \quad r < R_{\alpha\beta} \ , \tag{2.21}$$

where

$$K_{\alpha\beta} = \int_{R_{\alpha\beta}}^{\infty} h^D_{\alpha\beta}(s)\, s^{-1} ds \ . \tag{2.22}$$

Following Wertheim,[5] the relations for $\hat{h}^D_{21}(r)$ and $h^{\Delta}_{21}(r)$ may be uncoupled by taking linear combinations

$$h^+_{\alpha\beta}(r) = [\hat{h}^D_{\alpha\beta}(r) + \tfrac{1}{2} h^{\Delta}_{\alpha\beta}(r)] - 3K_{\alpha\beta} \ , \tag{2.23}$$

$$h^-_{\alpha\beta}(r) = [\hat{h}^D_{\alpha\beta}(r) - h^{\Delta}_{\alpha\beta}(r)] - 3K_{\alpha\beta} \ . \tag{2.24}$$

with analogous expressions for $c^+_{\alpha\beta}(r)$ and $c^-_{\alpha\beta}(r)$. The closure conditions (2.20) when applied to Eqs. (2.23) and (2.24) are equivalent to

$$h^+_{\alpha\beta}(r) = -1 \ , \quad r < R_{\alpha\beta} \ . \tag{2.25}$$

On using the linear combinations $h^+_{\alpha\beta}(r)$ in Eqs. (2.16) and (2.17), one finds

$$h^+_{21}(r) = c^+_{21}(r) + \sum_{\gamma=1}^{2} K_{\gamma 1} \rho^+_{\gamma} h^+_{2\gamma} * c^+_{\gamma 1} \ , \tag{2.26}$$

where $\rho^+_{\gamma} = 2\rho_{\gamma}$, $\rho^-_{\gamma} = -\rho_{\gamma}$. Equations (2.15) and (2.26) resemble the Ornstein–Zernike relations for a binary fluid, in which the molecular interactions are spherically symmetrical.

In the limit $R_2 \to \infty$, Eq. (2.19) together with Eqs. (2.23) and (2.24) yields

$$h^D_{21}(z) = [2h^+_{21}(z) - h^-_{21}(z) - 3] K_{21} \ . \tag{2.27}$$

As $\rho_2 \to 0$, Eqs. (2.15) and (2.26) reduce to

$$h^s_{21}(r) = c^s_{21}(r) + \rho_1 h^s_{21} * c^s_{11} \tag{2.28}$$

and

$$h^+_{21}(r) = c^+_{21}(r) + K_{11} \rho^+_1 h^+_{21} * c^+_{11} \ , \tag{2.29}$$

which can be written in bipolar coordinates as

$$h^+_{21}(r) = c^+_{21}(r) + \frac{2\pi K_{11} \rho^+_1}{r} \int_0^{\infty} dt\, t\, h^+_{21}(t) \int_{|r-t|}^{r+t} ds\, s\, c^+_{11}(s) \ . \tag{2.30}$$

On substituting $r = R_2 + z$, $t = R_2 + y$ and on taking the wall limit $R_2 \to \infty$, we find, for $z > 0$,

$$h^+_{21}(z) = c^+_{21}(z) + 2K_{11} \pi \rho^+_1 \int_{-\infty}^{z} dy\, h^+_{21}(y) \int_{|z-y|}^{\infty} ds\, s\, c^+_{11}(s) \ , \tag{2.31}$$

where z is the distance of the center of the dipolar hard sphere from the wall. The integral between the limits $-\infty$ and ∞ may be simplified by noting that $h_{21}(y) = -1$, when $-\infty < y < 0$, and in addition $|z-y| = z - y$, when $z > 0$ and $-\infty < y < 0$. On changing the order of integration between $-\infty$ and 0,

$$\int_{-\infty}^{0} dy\, h^+_{21}(y) \int_{|z-y|}^{\infty} ds\, s\, c^+_{11}(s) = \int_{z}^{\infty} ds (z-s)\, s c^+_{11}(s) \ . \tag{2.32}$$

Defining the functions

$$B^+(z) = \int_0^z c^+_{11}(s)\, s\, ds \ , \quad D^+(z) = \int_0^z c^+_{11}(s)\, s^2 ds \ , \tag{2.33}$$

the wall–particle + equations become

$$h^+_{21}(z) = c^+_{21}(z) + 2\pi K_{11} \rho^+_1 \{z\, [B^+(\infty) - B^+(z)] - [D^+(\infty) - D^+(z)]\} + 2\pi K_{11} \rho^+_1 \int_0^{\infty} dy\, h^+_{21}(y)\, [B^+(\infty) - B^+(|z-y|)] \ . \tag{2.34}$$

where the functions $B^+(z)$ and $D^+(z)$ are entirely determined by the interactions between the particles in the bulk fluid. An analogous equation can be written for the angularly independent part of the wall–particle total correlation function

$$h^s_{21}(z) = c^s_{21}(z) + 2\pi \rho_1 \left\{ z\, [B^s(\infty) - B^s(z)] - [D^s(\infty) - D^s(z)] + \int_0^{\infty} dy\, h^s_{21}(y)\, [B^s(\infty) - B^s(|z-y|)] \right\} , \tag{2.35}$$

where $B^s(z)$ and $D^s(z)$ have definitions which correspond exactly to $B^+(z)$ and $D^+(z)$.

In Eqs. (2.34) and (2.35), $\{c^s_{21}(z),\ c^s_{11}(s)\}$ and $\{c^+_{21}(z),\ c^+_{11}(s)\}$ are sets of two different, but consistent, direct correlation functions with corresponding closures (discussed in the next section) for the wall–particle and particle–particle interactions, respectively. The functions $c^s_{11}(r)$ and $c^+_{11}(r)$ for the bulk fluid particles are obtained in an independent calculation from

$$h^s_{11}(r) = c^s_{11}(r) + \rho_1 h^s_{11} * c^s_{11} \ , \tag{2.36}$$

$$h^+_{11}(r) = c^+_{11}(r) + K_{11} \rho^+_1 h^+_{11} * c^+_{11} \ , \tag{2.37}$$

which are the one-component analogs of Eqs. (2.28) and (2.29) first derived in a seminal paper by Wertheim. These equations carry their own closures for $h_{11}(r)$ ($r < R_{11}$) and $c_{11}(r)$ ($r > R_{11}$). We do not actually solve Eqs. (2.36) and (2.35) since nearly exact results are available from the work of Verlet and Weis[6] for hard spheres and from the study of Waisman, Henderson, and Lebowitz[7] for hard spheres against a wall. Our RLHNC approximation (Sec. III) implies that $h^s_{21}(z)$ is the exact wall–particle total correlation function for hard spheres against a hard wall. Equation (2.37) has been solved by Wertheim, in the mean spherical approximation,[6] while Patey and his colleagues have treated it in the LHNC and QHNC approximations,[8] using the Verlet–Weis theory for the hard-sphere interactions. We are therefore left with the necessity of solving only Eq. (2.34) under the appropriate closures for the wall–particle and particle–particle direction correlation functions.

The constants K_{11} and K_{21} determine the dipole moment m_1 and the electric field $\mathbf{E}_2$ through the relations

$$\frac{4\pi m^2_1 \rho_1}{3kT} = Q_+(2K_{11}\rho_1 R^3_{11}) - Q_-(-K_{11}\rho_1 R^3_{11}) \tag{2.38}$$

and

$$\frac{m_1 E_0}{kT} = K_{21} [2Q_+(2K_{11}\rho_1 R^3_{11}) + Q_-(-K_{11}\rho_1 R^3_{11})] \ , \tag{2.39}$$

where k and T are the Boltzmann constant and absolute temperature, respectively, and $Q_{\pm}(\rho_1 R^3_{11})$ is defined by:

$$Q_{\pm}(\rho_1 R^3_{11}) = 1 - 4\pi\rho_1 \int_0^{\infty} c^{\pm}_{11}(r, \rho_1)\, r^2 dr \ . \tag{2.40}$$

Equation (2.38) has been derived by Wertheim[5] in the mean spherical approximation, but its extension to the LHNC (or RLHNC) approximation is straightforward; nevertheless we present it for completeness and as a prelude to the derivation of (2.39), which Isbister and Fraser[1] discussed in the mean spherical approximation. The derivation of Eq. (2.38) rests on the asymptotic form of $c^D_{11}(r)$ [see Eqs. (3.1) and (3.6)]

$$c_{11}^D(r) \to \frac{2\pi\rho_1^2}{r^3} D(2,1) \ , \quad \text{as } r \to \infty \ . \tag{2.41}$$

On inserting this in

$$\hat{c}_{11}^D(r) = c_{11}^D(r) - 3\int_r^\infty ds\, s^{-1} c_{11}^D(s) \ , \tag{2.42}$$

one sees that $\hat{c}_{11}^D(r)$ is short ranged and tends to zero as $r \to \infty$:

$$\hat{c}_{11}^D(r) \to 0 \ , \quad \text{as } r \to \infty \ . \tag{2.43}$$

When the inverse relation [cf. Eqs. (2.19) and (2.18)]

$$c_{11}^D(r) = \hat{c}_{11}^D(r) - \frac{3}{r^3}\int_0^r \hat{c}_{11}(s)\, s^2 ds \tag{2.44}$$

is taken to the limit $r \to \infty$, one also finds that

$$\frac{m_1^2}{kT} = -3\int_0^\infty \hat{c}_{11}^D(s)\, s^2 ds$$
$$= -3K_{11}\int_0^\infty [2c_{11}^*(s, 2K_{11}\rho_1) + c_{11}^*(s, -K_{11}\rho_1)]\, s^2 ds \ , \tag{2.45}$$

where we have used the analogs of Eqs. (2.23) and (2.24) applied to $\hat{c}_{11}^D(s)$ in the last step. The result given in Eq. (2.38) follows immediately on applying Eq. (2.40).

The relation between K_{21} and E_0 is also derived from the asymptotic from of $c_{21}^D(r)$ in the MS and LHNC approximations [see Eqs. (3.1) and (3.6) in Sec. III]. The equation for dipolar mixtures which corresponds to Eq. (2.45) is[9]

$$\lim_{r_{21}\to\infty} \frac{m_2 m_1}{r_{21}^3 kT} = -\lim_{r_{21}\to\infty} \frac{3K_{21}}{r_{21}^3}\int_0^{r_{21}} [2c_{21}^*(s) + c_{21}^-(s)]\, s^2 ds \ , \tag{2.46}$$

where we have not canceled the r_{21}^3 in the denominator, because we intend to take the wall limit. Substituting $r_{21} = R_2 + z$, and taking the limit $R_2 \to \infty$, reduces the left hand side of Eq. (2.46) to $m_1 E_0/kT$, and replaces the upper limit of the integral in Eq. (2.46) by ∞. The Fourier transform of Eq. (2.29), which is an Ornstein–Zernike equation for mixtures, as $\rho_2 \to 0$, yields

$$\tilde{c}_{21}^*(k) = [1 - K_{11}\rho_1^* \tilde{c}_{11}^*(k)]\, \tilde{h}_{21}^*(k) \ , \tag{2.47}$$

from which, when $k = 0$, we have

$$\int_0^\infty c_{21}^*(s)\, s^2 ds = [1 - K_{11}\rho_1^* \tilde{c}_{11}^*(0)] \int_0^\infty h_{21}^*(s)\, s^2 ds \ . \tag{2.48}$$

In the above, the "~" represents the three dimensional Fourier transform

$$\tilde{t}(k) = \int d\mathbf{r} \exp(i\mathbf{k}\cdot\mathbf{r})\, t(|\mathbf{r}|) \ ,$$

and $t \equiv c$ or h.

Since $h_{21}^*(s)$ is a short-ranged function equal to -1 for $s < R_{21}$, it readily follows that

$$\lim_{R_2\to\infty} \frac{1}{r_{21}^3}\int_0^\infty h_{21}^*(s)\, s^2 ds = -\tfrac{1}{3} \ . \tag{2.49}$$

Hence,

$$\frac{m_1 E_0}{kT} = K_{21}[2[1 - K_{11}\rho_1^* \tilde{c}_{11}^*(0)] + [1 - K_{11}\rho_1^* \tilde{c}_{11}^-(0)]] \ , \tag{2.50}$$

which is identical to Eq. (2.39). It should be emphasized that Eqs. (2.36) and (2.39) are relations derived from the asymptotic forms of c_{11}^L and c_{21}^L in the MS and LHNC approximations. The dipole moment m_1 and the electric field E_2 are determined from K_{11} and K_{21}, after the solutions to Eq. (2.37) have been obtained.

The constant K_{21} also retrieves the coefficients $h_{21}^D(z)$ and $h_{21}^\Delta(z)$, which appear in the invariant expansion of the wall–particle correlation functions

$$h_{21}(z, E_2, \Omega_1) = h_{21}^\Delta(z) + h_{21}^D(z) D(2,1) + h_{21}^\Delta(z)\Delta(2,1) \tag{2.51}$$

by inverting Eq. (2.23) and (2.24) and using Eq. (2.27). Both $h_{21}^\Delta(z)$ (for the closure rules considered in the next section) and $h_{21}^\Delta(z)$ are short-ranged functions and tend to zero as $z \to \infty$, and the asymptotic form of $h_{21}^D(z)$ is therefore

$$\lim_{z\to\infty} h_{21}^D(z) = 3K_{21} \ , \tag{2.52}$$

which follows from Eq. (2.27) and the fact that $h_{21}^\Delta(z)$ is also short ranged. The asymptotic form of the wall–particle correlation function for the RLHNC closure, discussed in the next section, coincides with that of the MS approximation[3] and is therefore given by

$$\lim_{z\to\infty} h_{21}(z, E_2, \Omega_1) = 3K_{21} D(2,1) \tag{2.53}$$

$$= \frac{3m_1 E_0 D(2,1)}{kT[2Q(2K_{11}\rho_1 R_{11}^3) + Q(-K_{11}\rho_1 R_{11}^3)]} \tag{2.54}$$

$$= \frac{3E_0^* D(2,1)}{T^*[2Q(2K_{11}\rho_1 R_{11}^3) + Q(-K_{11}\rho_1 R_{11}^3)]} \ , \tag{2.55}$$

where

$$T^* = \left(\frac{kTR_{11}^3}{m_1^2}\right) \tag{2.56}$$

and

$$E_0^* = \frac{E_0 R_{11}^3}{m_1} = \frac{|\mathbf{E}_2|}{(3\cos^2\theta_2 + 1)^{1/2}} \frac{R_{11}^3}{m_1} \ . \tag{2.57}$$

Since the electric field is independent of the distance from the wall, $h_{21}(z, E_2, \Omega_1)$ does not decrease to zero as $z \to \infty$, unless the magnitude of the electric field or $D(2,1)$ is also zero. The angular average of $h_{21}(z, E_2, \Omega_1)$ is however zero in the limit $z \to \infty$:

$$\lim_{z\to\infty} \int h_{21}(z, E_2, \Omega_1)\, d\Omega_1 = 0 \tag{2.58}$$

since the angular averages of $D(2,1)$ and $\Delta(2,1)$ are zero and

$$\lim_{z\to\infty} h_{21}^s(z) = 0 \ . \tag{2.59}$$

We shall now consider the details of these equations in the context of the mean spherical and linearized hypernetted chain closure rules.

III. THE CLOSURE RELATIONS

The closures for the wall–particle direct correlation functions are readily derived by taking the wall limit of the corresponding closures in the bulk fluid.

A. MSA

The closure for the direct correlation function is

$$c_{\alpha\beta}(r) = -\frac{m_\alpha m_\beta}{kT r^3} D(1,2) \ , \quad \text{for } r > R_{\alpha\beta} \ , \tag{3.1}$$

which is equivalent to

$$c^s_{\alpha\beta}(r) = 0 \ , \quad \text{for } r > R_{\alpha\beta} \ . \tag{3.2}$$

This is unaffected, for $r > R_{21}$, on taking the wall limit of $c^s_{21}(r)$.

B. LHNC approximation

Starting with the hypernetted chain (HNC) approximation

$$c_{\alpha\beta}(2,1) = h_{\alpha\beta}(2,1) - \ln g_{\alpha\beta}(2,1) - V_{\alpha\beta}(2,1)/kT \quad (r > R_{\alpha\beta}) \tag{3.3}$$

and using the invariant expansions of $c_{\alpha\beta}(2,1)$ and $h_{\alpha\beta}(2,1)$ [cf. Eqs. (2.13) and (2.14)], one finds

$$c^s_{\alpha\beta}(r) = h^s_{\alpha\beta}(r) - \ln\left[g^s_{\alpha\beta}\frac{\left[1 + \hat{b}^D_{\alpha\beta}(r) D(2,1) + \hat{b}^\Delta_{\alpha\beta}\Delta(2,1)\right]}{g^s_{\alpha\beta}(r)}\right] - \frac{V^s_{\alpha\beta}(r)}{kT} - \frac{m_\alpha m_\beta}{kT r^3} D(2,1) \ , \tag{3.4}$$

where $V^s_{\alpha\beta}$ is the spherically symmetric part of the potential. Expanding the logarithm up to the linear term, and collecting and comparing coefficients of 1, $D(2,1)$, and $\Delta(2,1)$, we have

$$c^s_{\alpha\beta}(r) = h^s_{\alpha\beta}(r) - \ln g^s_{\alpha\beta}(r) - V^s_{\alpha\beta}(r)/kT \ , \tag{3.5}$$

$$c^D_{\alpha\beta}(r) = h^D_{\alpha\beta}(r)\left[1 - g^s_{\alpha\beta}(r)^{-1}\right] - \frac{m_\alpha m_\beta}{r^3 kT} \ , \tag{3.6}$$

$$c^\Delta_{\alpha\beta}(r) = h^\Delta_{\alpha\beta}(r)\left[1 - g^s_{\alpha\beta}(r)^{-1}\right] \ . \tag{3.7}$$

Defining

$$b^D_{\alpha\beta}(r) = h^D_{\alpha\beta}(r)\left[1 - g^s_{\alpha\beta}(r)^{-1}\right] \ , \tag{3.8}$$

$$b^\Delta_{\alpha\beta}(r) = h^\Delta_{\alpha\beta}(r)\left[1 - g^s_{\alpha\beta}(r)^{-1}\right] \ , \tag{3.9}$$

with $\hat{b}^D_{\alpha\beta}(r)$ and $b^*_{\alpha\beta}(r)$ also defined by equations analogous to Eqs. (2.18), (2.23), and (2.24), respectively, the last two equations can be written in the form

$$c^*_{\alpha\beta}(r) = b^*_{\alpha\beta}(r) \ , \quad r > R_{\alpha\beta} \ . \tag{3.10}$$

In the RLHNC, Eq. (3.5) is replaced by the exact closure for hard spheres against a wall.

In the wall limit, $\hat{b}^D_{21}(z) = b^D_{21}(z)$, and making use of Eq. (2.27), the closure condition for the wall–particle direct correlation function becomes

$$c^s_{21}(z) = \left[1 + h^s_{21}(z)\right]\left[1 - g^s_{21}(z)^{-1}\right] \ , \quad z > 0 \ . \tag{3.11}$$

On substituting this in Eq. (2.34), we have, for $z > 0$,

$$h^s_{21}(z) = \left[g^s_{21}(z) - 1\right] + g^s_{21}(z)\, 2\pi K_{11}\rho^*_1 \left\{ z\left[B^*(\infty) - B^*(z)\right] + \left[D^*(\infty) - D^*(z)\right] + \int_0^\infty h^s_{21}(z)\left[B^*(\infty) - B^*(|z-y|)\right] dy \right\} . \tag{3.12}$$

When $g^s_{21}(z) = 1$, the formal equation for $h^s_{21}(z)$ in the MSA approximation is recovered.

The above equations (3.12) were solved iteratively on a computer to generate the accompanying figures.

IV. RESULTS AND DISCUSSION

The solution of Eq. (2.51), for $h_{21}(z, E_2, \ldots)$, was obtained as the confluence of three distinct computations.

(1) The bulk correlation functions were calculated in the manner described by Patey, from Eq. (2.37). The reduced dipole moment dependence of this relation is contained in the constant K_{11}, through Eq. (2.38), that also be expressed in the MSA and RLHNC approximations as

$$\rho^{*2}_1 = \frac{m^{*2}_1}{kT R^3_{11}} - c^D_{11}(R^*_{11}) - b^D_{11}(R^*_{11}) \ , \tag{4.1}$$

where $c^D_{11}(R^*_{11})$ and $b^D_{11}(R^*_{11})$ are the values of $c^D_{11}(r)$ and $b^D_{11}(r)$ immediately outside contact. The value of K_{11} was adjusted until this difference assumed the desired reduced dipole moment. The iteration of Eq. (2.37) was performed using fast Fourier transform techniques and mixed solutions to speed convergence. The bulk fluid correlation functions obtained showed excellent agreement with those of Patey.[8]

(2) The electric field which emerges from the wall was determined by Eqs. (2.9), (2.39), and (2.40). The field angle α_1 of Fig. 1 was taken, in separate calculations, as 0°, 45°, and 90°. The field angle is related to the wall–dipole orientation θ_2 through Eq. (2.10), the solution of which appears in Fig. 1. The magnitude of the reduced electric field

$$E^*_2 = -\frac{\mathbf{E}_2 R^3_{11}}{m_1} = \frac{E_0(3\cos^2\theta_2 + 1)^{1/2} R^3_{11}}{m_1} \tag{4.2}$$

was taken, as in the earlier work of Isbister and Freasier, to be 8/3, with the reduced dipole moment squared m^{*2}_1 fixed at either 0.5 or 1.0. For purposes of comparison of these parameters to a molecular system, the reduced dipole moment squared for HCl ($m_1 = 1.03$ D) at 275 °K, assuming a diameter of 3.5 Å, is approximately 0.65. A reduced field strength of 8/3 for this system corresponds to an electric field of nearly 1.9×10^9 V/m or a surface charge density σ of 1 electronic charge/1000 Å^2.

We have also carried out calculations at the same surface charge density (or electric field E_2) for a fluid at a reduced density of 0.7 with the reduced dipole moment $m^*_1 = 2.0$. These numbers correspond approximately to those appropriate for liquid water ($m_1 = 1.85$ D, $R_{11} = 2.76$ Å) at room temperature. The reduced electric field E^*_2 [which contains m_1 and R^3_{11} in its definition (4.2)] is now only 0.71. (It may be useful for the reader to bear in mind that it is an artifact of our definition of E^*_2 that an increase in the dipole moment m_1 results either in a reduction of E^*_2 when the surface charge density is held constant, or an increase in the surface charge density when E^*_2 is unchanged.)

(3) The spherically symmetric part of Eq. (2.51), i.e., $h^s_{21}(z)$, was determined using the technique of Waisman, Henderson, and Lebowitz.[7] The function $h^s_{21}(z)$ was first obtained from Eq. (2.28) as the Percus–Yevick solution and then corrected to produce an essen-

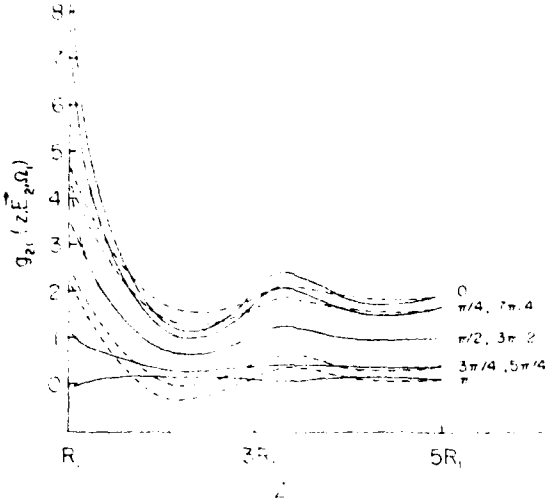

FIG. 2. The wall–particle distribution functions $g_{21}(z, \mathbf{E}_2, \Omega_1)$ as a function of the distance z from the wall for different orientations Ω_1 of the fluid dipoles where $E_2^* = 8.3$, $m_1^{*2} = 0.5$, $\rho^* = 0.573$, and $\alpha_1 = 0$. R_1 is the radius of a fluid dipole. —— RLHNC approximation, ----- MS approximation.

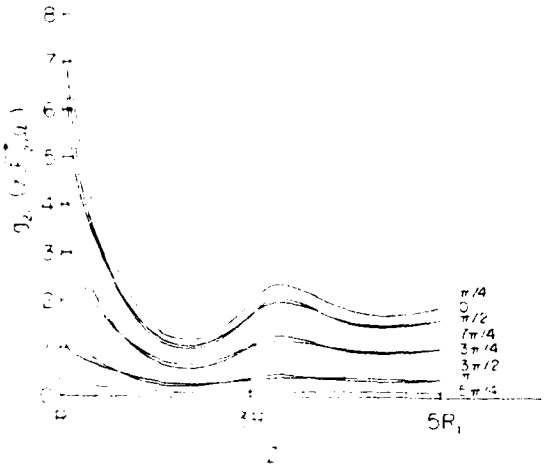

FIG. 3. Wall–particle distribution functions for the system depicted in Fig. 2 except that $\alpha_1 = 45°$.

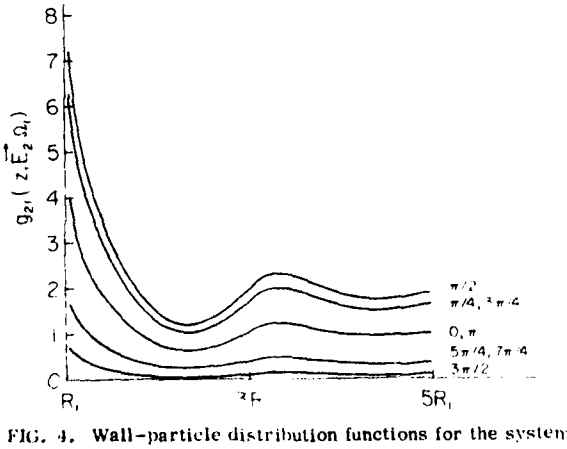

FIG. 4. Wall–particle distribution functions for the systems depicted in Figs. 2 and 3 except that $\alpha_1 = 90°$.

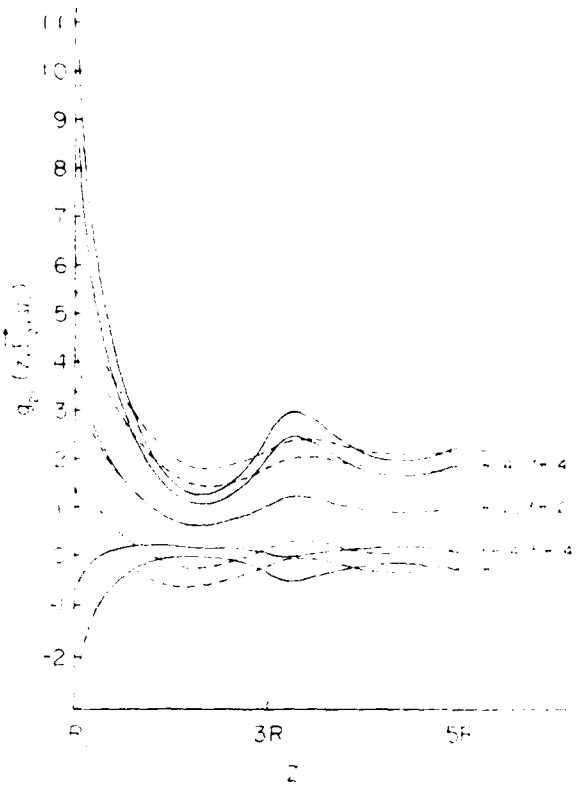

FIG. 5. The wall–particle distribution function $g_{21}(z, \mathbf{E}_2, \Omega_1)$ for the system depicted in Fig. 1 except that $m_1^{*2} = 1.0$.

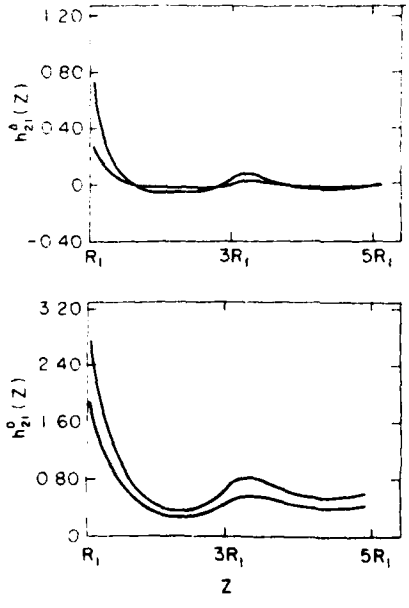

FIG. 6. The expansion coefficients $h_{00}^{\Delta}(z)$ and $h_{00}^{D}(z)$ as a function of the wall–particle distance z when $E_2^* = 8.3$ and $\rho^* = 0.573$. The upper and lower curves, in each case, are for $m_1^{*2} = 1.0$ and 0.5, respectively.

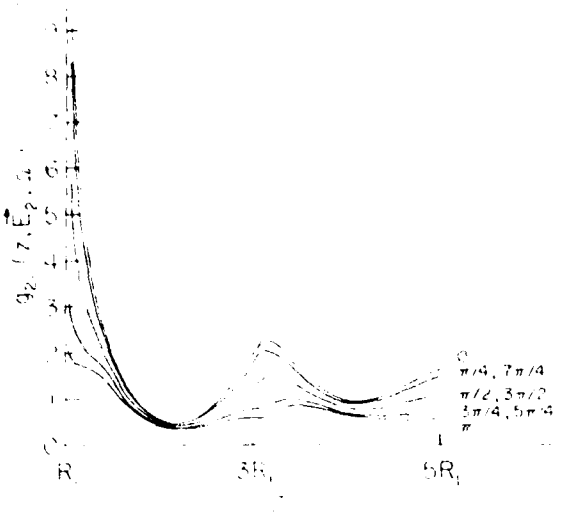

FIG. 7. The wall–particle distribution function $g_{21}(z, \mathbf{E}^*, \Omega_1)$ as a function of the distance z from the wall, for different orientations Ω_1 of the fluid dipoles when $E^* = 0.71$, $m_1^{*2} = 1.0$, $\rho_1^* = 0.7$, and $\sigma_2 = 0$. The reduced parameters m_1^* and ρ_1^* are those appropriate for liquid water at room temperature ($m_1 = 1.85$ D, $R_{11} = 2.76$ Å). The reduced electric field $E^* = 0.71$ corresponds to a surface density of 1 electronic charge/1000 Å^2.

tially exact wall–particle correlation function in comparison to Monte Carlo simulation. The reduced density of hard spheres, upon which $h_{21}^{\delta}(z)$ depends solely, was taken as $\rho^* = \rho_1 R_{11}^3 = 0.573$.

The computations were combined through Eqs. (2.23), (2.24), and (3.12) to yield the coefficients of the angular functions of Eq. (2.51). The integrals over bulk correlation functions (2.33) as well as the integral of Eq. (3.12) were performed by trapezoidal approximation. The iterative solution to Eq. (3.12) was rapidly convergent. Finally, the expansion coefficients were inserted into Eq. (2.51).

In Figs. 2–5 we present our results for $g_{21}(z, \mathbf{E}_2, \Omega_1)$ in the RLHNC approximation. The expansion coefficients $h_{21}^{D}(r)$ and $h_{21}^{\Delta}(r)$ are shown in Fig. 6. A comparison of RLHNC and MSA results, for a field angle of zero and reduced dipole moment squared of 0.5 and 1.0, are shown in Figs. 2 and 5, respectively.

In the case of $m_1^{*2} = 0.5$, $E_2^* = 8.3$, and $\rho_1^* = 0.573$ $g_{21}(z, \mathbf{E}_2, \Omega_1)$ in the RLHNC approximation assumes negative values only very near and at contact for a dipole orientation in opposition to the field. For higher values of $m_1^{*2} = 1.0$, at the same reduced electric field and fluid density, these regions are more pronounced and extended in range (Fig. 5). An increase in m_1^{*2} from 0.5 to 1.0 at constant E_2^* and ρ_1^*, however, corresponds to a fourfold increase in the surface charge density from 1 electronic charge/1000 Å^2 to one every 250 Å^2. Both the RLHNC and MSA treatments result in distributions showing enhanced adsorption for favorable dipole orientations, but the repulsive interactions of the electric field with unfavorably aligned dipoles is more clearly visible in the RLHNC approximation. This theory, like the MSA, is essentially linear in character, and cannot prevent the distribution functions from becoming negative when the dipoles are aligned against the field, if at the same time the theory predicts a large enhancement of the adsorption of dipoles aligned with the field. When, for example, the electric field is perpendicular to the wall, both theories predict that the density profiles (see Figs. 2 and 5) are symmetrical about the profile for dipoles perpendicular to the field (i.e., $\pi/2$ or $3\pi/2$). A large enhancement of dipoles aligned with the field would lead to an equally large depletion of dipoles oriented against the field, which may require negative wall–particle distribution functions. Further improvements beyond the RLHNC approximation would then be necessary. Figure 7 shows, however, that the RLHNC theory provides plausible density profiles even when the square of the dipole moment m_1^{*2} is increased to 4.0 but the surface charge density is maintained at 1 electronic charge/1000 Å^2.

ACKNOWLEDGMENTS

Support from the National Science Foundation, Contract No. CHE 77-10023, and from the Office of Naval Research, Contract No. N00014 78-c-0724 are gratefully acknowledged. One of us (D.I.) would like to thank the University of New South Wales for a leave of absence, and the Australian Research Grants Commission for its assistance.

[1] D. J. Isbister and B. C. Freasier, J. Stat. Phys. 20, [illegible] (1979). The notation that is used in this paper is slightly different. In particular, R_α is the radius of the α species rather than the diameter, and $E_\sim$ and $E_\perp$ as defined here are $E_\parallel$ and $E_\perp$, respectively, of Isbister and Freasier. The LHNC approximation for dipolar fluids proposed by G. N. Patey [Mol. Phys. 34, 427 (1977)] is identical to the single superchain approximation suggested earlier by M. S. Wertheim [Mol. Phys. 26, 1425 (1973)]. The analog of this approximation for the wall–particle closure is used in this study.
[2] G. Stell and J. J. Weis, Phys. Rev. A 21, 616 (1980).
[3] F. Helland, H. Reiss, H. L. Frisch, and J. L. Lebowitz, J. Chem. Phys. 33, 1379 (1960); see also J. W. Perram and E. R. Smith, Proc. R. Soc. (London) Ser. A 353, 193 (1977).
[4] M. S. Wertheim, J. Chem. Phys. 55, 4291 (1971).
[5] L. Verlet and J. J. Weis, Phys. Rev. A 5, 939 (1972).
[6] E. Waisman, D. Henderson, and J. L. Lebowitz, Mol. Phys. 32, 1373 (1976).
[7] G. N. Patey, Mol. Phys. 34, 427 (1977); G. N. Patey, D. Levesque, and J. J. Weis, Mol. Phys. 38, 1635 (1979).
[8] (a) D. Isbister and R. J. Bearman, Mol. Phys. 28, 1297 (1974); 32, 597 (1976); (b) D. Isbister, Mol. Phys. 32, 949 (1976).

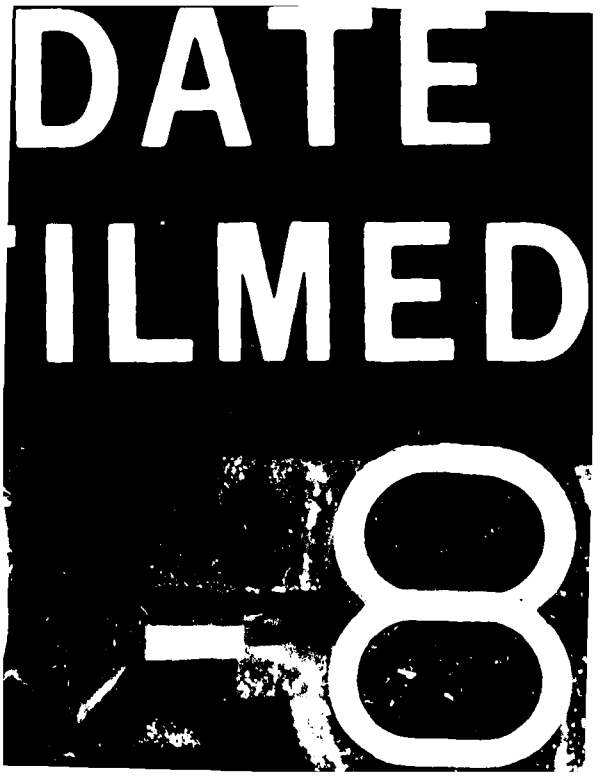
DATE
ILMED
-8